Bone 50 (2012) 343–349

Contents lists available at SciVerse ScienceDirect

Bone

journal homepage: www.elsevier.com/locate/bone

Case Report

A novel splicing mutation in FKBP10 causing osteogenesis imperfecta with a possible mineralization defect

Giacomo Venturi [a,1], Elena Monti [a,1,*], Luca Dalle Carbonare [b], Massimiliano Corradi [a], Alberto Gandini [a], Maria Teresa Valenti [b], Attilio Boner [a], Franco Antoniazzi [a]

[a] Department of Life and Reproduction Sciences, Pediatric Clinic, University of Verona, Italy
[b] Department of Internal Medicine — Section D, University of Verona, Italy

ARTICLE INFO

Article history:
Received 10 November 2010
Revised 6 October 2011
Accepted 24 October 2011
Available online 30 October 2011

Edited by: Richard Eastell

Keywords:
Bone
Fractures
Biphosphonate
Collagen
FKBP10
COL1A1

ABSTRACT

Osteogenesis imperfecta (OI) is a group of hereditary disorders characterized by bone fragility and osteopenia, with a broad spectrum of clinical severity. The majority of cases are dominantly inherited and due to mutations in type I collagen genes, whereas recessive forms are less frequent and attributable to mutations in different genes involved in collagen I post translational modifications and folding (prolyl-3-hydroxylase complex, *SERPINH1*, *FKBP10*).

We report the case of a patient with an initially mild and then progressively severe form of osteogenesis imperfecta due to a novel homozygous splicing mutation in *FKBP10* (intron 8 c.1399+1G>A), which results in aberrant mRNA processing and consequent lack of FKBP65 chaperone.

Although this mutation does not affect collagen type I post translational modifications in dermal fibroblasts, the histomorphometric pattern of our patient's bone sample showed a mineralization defect possibly due to the mutation in *FKBP10*.

Introduction

Osteogenesis imperfecta (OI) is a heterogeneous disorder characterized by evidence of malfunctioning connective tissue [1]. Clinical severity varies widely and patients suffer various degrees of bone fragility (from mild osteopenia to progressive skeletal deformities due to recurrent fractures), short stature (from normal to severely compromised height), sclerae that vary from blue to white coloration and dental abnormalities (such as dentinogenesis imperfecta).

Before genetic causes were identified, Sillence classified four OI types based on mode of inheritance and on clinical and radiological criteria: the mild non-deforming type I, the perinatal lethal type II, the severely deforming type III and the moderately deforming type IV. In the 1980s, all of these OI forms were explained by heterozygous mutations in one of the two genes encoding type I collagen (MIM 120150 and 120160), the major component of bone, tendons and skin, with both quantitative (milder, *COL1A1*) and qualitative (moderate to lethal, *COL1A1* and *COL1A2*) defects in the synthesis of the protein [2–4]. Moderate to severe OI cases, without COL1 gene mutations and with recessive or unclear heredity, were observed and classified later on the basis of distinct clinical and bone histological features as types V and VI. The former is a presumably dominant form characterized by dense metaphyses, hypertrophic callus formations, early calcification of the interosseous membrane at the forearm and mesh-like bone lamellation on histological examination; the latter is characterized by disordered mineralization, with usually high alkaline phosphatase (ALP) values, an augmented osteoid, fish-scale pattern of lamellation and with autosomal recessive heredity [5]. In recent years, the molecular bases of other recessive forms of OI have been described, and today it is known that some of these heterogeneous disorders are caused by defects in genes coding for proteins involved in proper collagen I post-translational modification and folding and in the regulation of osteoblast differentiation [6–11]. Mutations in *CRTAP-LEPRE1-PPIB* genes, encoding the prolyl-3-hydroxylation complex, which is responsible for α1(I) Pro986 residue hydroxylation, affect post-translational modification and folding with a typical lack (or reduction) of 3HyP and extensive lysyl hydroxylation and glycosylation of pro α chains in the ER, presumably because of delayed folding of trimers. Null mutations in *CRTAP* (MIM 605497) and *LEPRE1* (MIM 610339) have been reported to cause severe to lethal forms of OI with typical rhizomelia [12–17], while mutations in *PPIB* (MIM 123841) have more variable clinical and biochemical outcomes, resulting in moderate to severe cases without rhizomelia,

* Corresponding author at: Life and Reproduction Sciences, Pediatric Clinic, University of Verona, Policlinico Giambattista Rossi, Piazza Ludovico Antonio Scuro, 10, I-37134 Verona, Italy. Fax: +39 045 8124790.
E-mail address: elena.monti@univr.it (E. Monti).
[1] Contributed equally to this work.

8756-3282/$ – see front matter © 2011 Elsevier Inc. All rights reserved.
doi:10.1016/j.bone.2011.10.023

and with impaired to normal α1(I)Pro986 hydroxylation and collagen helix modification [18,19]. Recently, new mutations have been found in the genes coding for the chaperones involved in the intracellular folding and trafficking of collagen triple helix. A *SERPINH1*/HSP47 (MIM 600943) homozygous missense mutation has been described as causing a severely deforming type of OI that is similar in severity to type III [20]; while mutations in the *FKBP10* gene (MIM 607063), which encodes FKBP65, an ER FK506-binding protein with peptidyl-prolyl cis–trans isomerase activity (PPIase) and chaperone function, have been found in patients whose bone biopsies showed thin lamellae and a pattern resembling fish scales [21].

We describe herein the case of a patient who had an initially mild and then progressively severe form of OI, in spite of the pharmacological and physiotherapy treatments [22–24], histologically showing possible mineralization defects due to an autosomal recessive mutation in *FKBP10*, not yet described in the literature.

Case report

The index case (O_137, internal code) is the second child born to healthy (Target height +1 SD), consanguineous Italian parents (See Appendix for the family pedigree). Family history was noncontributory and prenatal history was uneventful. The boy was born at term by induced labor; he weighed 3400 g (40th percentile) at birth and was 50 cm (40th percentile) in length. At birth he responded well, although a displaced fracture of the clavicle with bilateral stretch of brachial plexus was reported. At 8 months of age the first pathological fractures were detected (right tibia greenstick fracture and pathological rib fractures). A mild motor development delay was suspected, so at 10 months bone and muscular biopsies were done which excluded histiocytosis X and a myopathy (data not available).

Subsequently, fractures after mild trauma became more frequent (6 fractures between 2 and 5 years of age). A physical examination at 4 years showed a phenotype resembling OI type I: the boy was short and thin (98 cm and 15.5 kg: both −1 SD) with white sclera, long fingers and toes, moderate small joint laxity but no arthrogryposis, dentinogenesis imperfecta or phenotypic anomalies. Biological data showed mild sideropenic anemia and bone-related enzymes within normal ranges, but with the exception of the C-terminal cross-linked telopeptide of type I collagen (CTX) that was extremely high. Radiologically we observed the presence of wormian bones in the skull (Fig. 1b), a progressive cortical width reduction in the long bones (Figs. 1a-g-h-i-l) and a flattening of a vertebral body with progressive scoliosis (Figs. 1c-d-e-f). At age 4.5 years, we started the child on biphosphonate (BP) therapy (Neridronate every 3 months

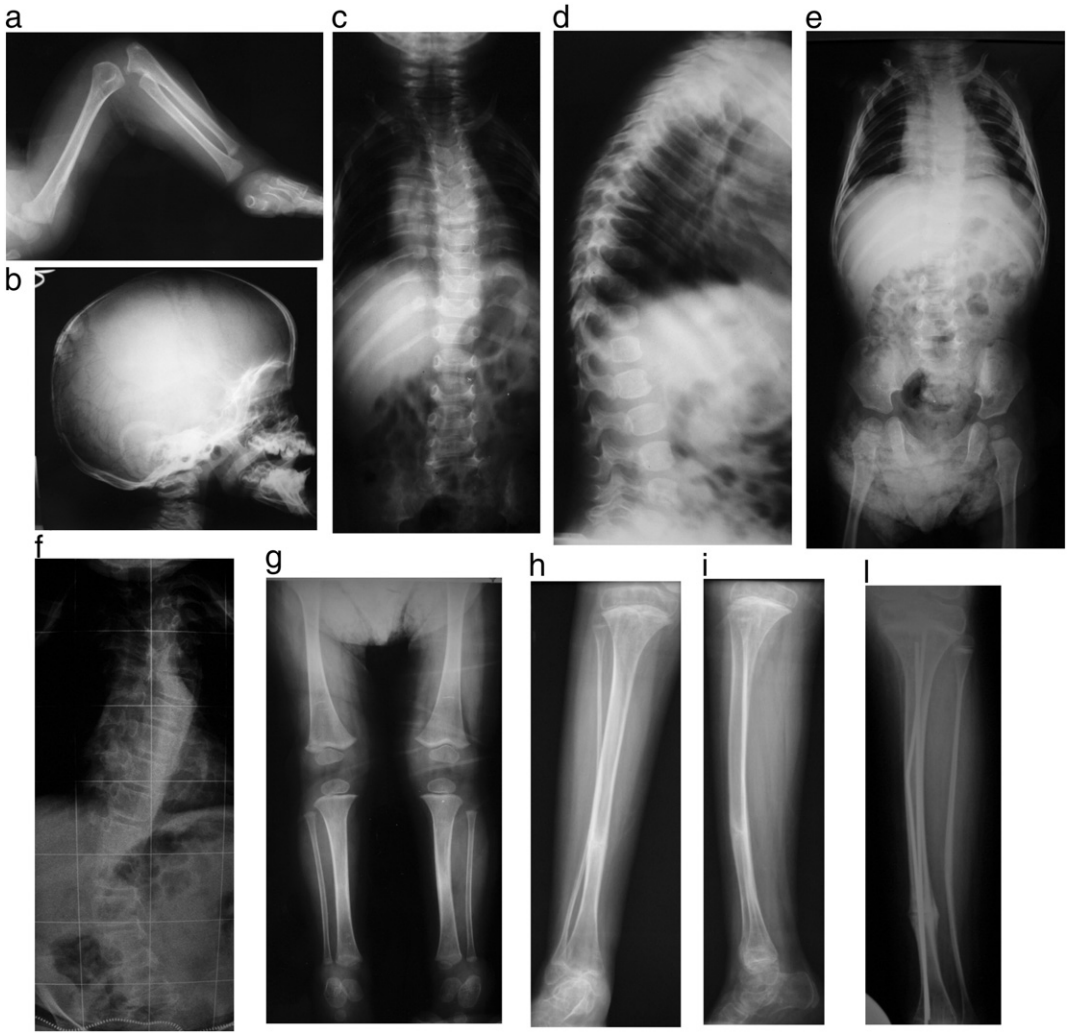

Fig 1. a. X-ray at birth of lower limbs showing substantially normal long bones. b: X-ray at 11 months of wormian bones at skull LL; c and d: X-ray at 11 months of trunk AP and LL, showing vertebrae plana and deformation; e: trunk and pelvis X-ray at 11 months in AP showing coxa valga; f: progressively severe scoliosis at 11.5 years old; g: lower limb X-ray showing slight reduction of cortical thickness at 11 months. h-i-l: extremely thin lower limbs at 11.5 years old.

at a dose of 2 mg/kg) together with calcium, 25-hydroxy-vitamin D (25-OHD) and iron supplements. Because of a concomitant low response to growth hormone (GH) stimulation tests (See Appendix), the boy has been undergoing GH treatment since the age of 7.5 years (113 cm and 23 kg, −2 SD and M, respectively). BP was administered continuously until the boy was 10 years old, when they were suspended for almost 1 year because of surgery; subsequently, he restarted therapy at half the standard dose (1 mg/kg) every 4 months for 1 year, when the dosage was increased to the standard dose. There were fewer fractures after 5 years of age (only 1 between 6 and 10 years). Physical check-ups remained non-contributory up to 8 years of age when the initially mild form turned to a moderately severe phenotype. The boy presented with short stature (117 cm and 29 kg, respectively −1/−2 SD and +1 SD), a short trunk due to gradually worsening kyphoscoliosis, with flattening and wedging of the vertebrae (Fig. 1f) that required a bivalve brace, and eventually genu valgum with normal extensibility of the joints. No hearing loss has been verified, but the patient developed mild prognatism and myopia. He started using a wheelchair by late childhood, but at home he is able to walk with assistance. The fracture rate increased following the suspension of therapy (5 between 11 and 12 years), but has since subsided. Now, at 13 years old, he is −1/−2 SD for height and +1/+2 SD for weight (140 cm and 47 kg, respectively) and surgery for spine stabilization has been scheduled.

Regarding biological data, ALP, as well as parathormone (PTH), 25OHD and calcium urinary secretion have remained within normal ranges, whereas CTX has always been above normal ranges. Radiographic assessment revealed that osteopenia was severe; subsequently, this parameter was followed by a six-month dual-energy X-ray absorptiometry (DXA) (See Appendix). A slight but steady increase in bone mineral density (aBMD) was observed during the first three years of BP therapy. Then progress slowed until GH was started, when we noticed a slight reactivation of the increase in aBMD, although, and more important, it seemed to stabilize the aBMD. In fact, when BP and GH were suspended because of surgery, the aBMD decreased even if there was no change in height velocity.

Methods

DNA extraction and quantification

Proband's genomic DNA (gDNA) was isolated from 400 µl of a peripheral whole-blood sample using a magnetic particle-based methodology via an automated purification procedure according to the manufacturer's instructions (Maxwell® 16 DNA Purification Kits, Promega Corporation; Madison, WI, USA). Accurate quantification of obtained gDNA was done by fluorimetric method (Qubit fluorometer, Invitrogen; Carlsbad, NM, USA).

PCR amplification

Coding regions and relative intronic bounderies of the FKBP10 gene were amplified by 10 specific intronic couples of primers (See Appendix) and each PCR reaction occurred in 25 µl final volume with 20 ng of gDNA, 400 nM of each primer, 200 µM of each dNTP (Invitrogen; Carlsbad, NM, USA), 1.5 mM $MgCl_2$, 5× Colorless Go Taq® Flexi Buffer and 1 U of Go Taq® Hot Start Polymerase (Promega Corporation; Madison, WI, USA). Following an initial 2-min denaturation step at 95 °C, 35 cycles were repeated consisting of 30 s at 95 °C, 30 s at each amplicon specific annealing temperature (range 62 °C–66 °C) and 30 s at 72 °C followed by a final extension time of 5 min at 72 °C. Amplification was performed on a gradient thermal cycler (Mastercycler epgradient, Eppendorf; Hamburg, Germany) and PCR product was checked for specificity and for quantification by electrophoretic migration on 2% agarose gel.

PCR product purification and sequence analysis

Amplified fragments were purified by a selective DNA/silica membrane binding reaction carried out on a column support (Illustra GFX PCR DNA and gel band purification kit, GE Healthcare; Buckinghamshire, UK); and 50 fmol of the same PCR product was used for the dye terminator cycle sequencing reaction with the CEQ DTCS Quick Start Kit (Beckman Coulter; Fullerton, CA, USA) according to the manufacturer's protocol. The sequencing reaction product was purified by ethanol precipitation, resuspended in a sample loading solution and analyzed with a capillary electrophoresis sequencer (CEQ 8800, Beckman Coulter; Fullerton, CA, USA).

qRT-PCR amplification

The expression of FKBP10 and COL1A1 in fibroblasts, which share a mesodermal origin with osteoblasts, was examined by means of a real-time reverse transcriptase polymerase chain reaction (qRT-PCR) and normalized to GAPDH and HPRT1 mRNA levels. Specifically, 500 ng of total extracted RNA were retrotrascripted with iScript cDNA Synthesis Kit and then 10 ng amplified with IQ SYBR Green Supermix on a IQ5 thermocycler (Bio-Rad Laboratories; Hercules, CA, USA). After an initial 3-min denaturation step at 95 °C, 40 cycles were repeated consisting of 10 s at 95 °C and 30 s at 60 °C.

Cell cultures

Dermal fibroblast cultures were established from explanted skin biopsies taken from the patient and from a normal individual (control) with appropriate consent and grown in high glucose DMEM (Euroclone, Italy) supplemented with 10% FBS, 2 mM L-glutamine, 100 U/ml penicillin and 100 µg/ml streptomycin. For each experiment, 250,000 cells were seeded into 35-mm dishes and left to grow for 1 day. Eighty percent confluent fibroblasts were then incubated for 24 h with DMEM supplemented with 1% FBS, 100 µg/ml ascorbic acid, L-glutamine, penicillin and streptomycin. Media and cell layers were collected from the dishes in the presence of protease inhibitors (Roche, Germany) on ice.

In vitro biochemical studies

Type I collagen secreted by patient and control fibroblasts were isolated as detailed elsewhere [25]. Ammonium sulfate precipitates of media and cell layer procollagens were digested with pepsin, fluorescently labeled with Cy5, denatured at 60 °C for 10 min and separated by SDS-PAGE on 0.5% urea gels (6% running, 4% stacking). Separated collagens were scanned with a Typhoon laser scanner and analyzed with ImageQuant 5.1 (GE Healthcare; Buckinghamshire, UK).

Western blot FKBP65

Control and patient cells were lysated in RIPA buffer supplemented with protease inhibitor cocktail (Roche, Germany), separated by SDS-PAGE on a 10% gel under reducing conditions and transferred to a pvdf membrane. Western blots were probed with two alternative clones of a monoclonal antibody against human-FKBP65 (M02-3B5 and M13 2D4, Abnova, Taiwan) and with an anti-α-tubulin antibody (Calbiochem, San Diego, CA, USA) as loading control. Reactive bands were revealed by chemiluminescence with secondary antibody conjugated with horseradish peroxidise (R&D Systems, Minneapolis, MN, USA).

Bone biopsy and histomorphometry

An iliac crest biopsy was taken at 13 years, at 6 months after suspension of 7 years of neridronate treatment, transiliac bone biopsy, taken from the iliac crest, was fixed in 70% ethanol and embedded undecalcified in methyl-methacrylate resin (Merck 800590, Germany). Bone sections were cut with a microtome (Polycut S, Leica Microsystems, Wetzlar, Germany) equipped with a carbide-tungsten blade, stained with Goldner's stain and toluidine blue and mounted on microscope slides for histomorphometric measurements. Some sections were left unstained for the measurement of fluorescent labeling. The sections were obtained from three different levels of the methyl-methacrylate block, each separated by a thickness of 250 μm. Histomorphometric results were calculated as the mean of the values obtained from the three different levels as an approximation of a 3-D evaluation. This also avoided replicating the sampling of any single bone remodeling unit.

Measurements were taken by means of an image analysis system consisting of an epifluorescent microscope (Leica DM2500) connected to a digital camera (Leica DFC420 C) and a computer equipped with a specific software for histomorphometric analyses (Bone 3.5, Explora Nova, France). Histomorphometric parameters were reported in accordance with the ASBMR Committee nomenclature [26].

Results

Identification of the mutation and FKBP10 expression

Complete sequencing of the *COL1A1*, *COL1A2*, *CRTAP*, *LEPRE1* and *SERPINH1* genes revealed the absence of any pathological nucleotidic variation.

The proband harbors a homozygous c.1399+1G>A mutation in the first of two strictly conserved nucleotides in the donor splice site of intron 8 inherited in a recessive manner from the healthy heterozygous parents (Fig. 3a). This variation results in the production of two different steady mRNA molecules as is shown by RT-PCR amplification (Fig. 3e): a first molecule (Fig. 3b) with complete skipping of exon 8, in which a shift in the reading frame generates a premature stop codon in exon 9 (p.His420ProfsX12); and a second longer molecule (Fig. 3c), where recognition of a cryptic donor site at position c.1303 causes the incorporation of a small fragment of exon 8 (first 46 bp) with a consequent shift in the reading frame and the introduction of a premature stop codon in exon 10 (p.Val435ProfsX64).

Gene expression analysis by real-time RT-PCR showed a reduced level of FKBP10 in the patient's fibroblasts compared to wild-type (0.465 fold, Fig. 3f), that could be explained by other different unstable splicing products, harboring a premature termination codon or by down-regulation of the same gene. Western blot analysis showed that protein product FKBP65 was undetectable in patient cells.

Collagen expression

COL1A1 expression, evaluated by qRT-PCR, revealed an increase in mRNA levels (2.188 fold; Fig. 3f), as if there was a compensative up-regulation of the collagen production in response to its delayed secretion [21]. On the other hand, gel electrophoresis of proband collagen I showed normal α1(I) and α2(I) amounts in media compared with healthy control cells. No evidence of alterations in electrophoretic chain migration (Figs. 2d–e) indicates that the FKBP10 mutation does not affect post translational modification in collagen type I.

Histological findings

Comparing the histomorphometric pattern of the patient's sample with those previously described [5,27], there is a poor, diffuse uptake of the tetracycline, under fluorescent light (Fig. 2b). Adjusted apposition rate, trabecular and osteoid thickness could be similar to type VI OI (Table 1); on the other hand, osteoid surface is more like normal controls and qualitative evaluation under polarized light showed a loss of the normal orientation of the lamellae with a osteomalacic pattern, confirmed by the mineralization lag time, that is here even longer than the full range for type VI OI. (Figs. 2a–c).

Discussion

We describe a patient with progressive OI, initially similar to a mild form and gradually evolving towards a moderately severe form, worsening both in terms of growth rate and number of fractures. The patient turned out to be affected by autosomal recessive OI due to a homozygous mutation in *FKBP10*. He is the only affected member in all of his extended family.

Interestingly, the OI phenotype previously described in association with *FKBP10* mutations seems more severe [21] than the one we describe here. Since none of the patients described in early works is reported to be taking BP, we believe that BP together with GH therapy in this case helped obtain steady state metabolism and better bone mass than would have occurred in the natural course of the disease, as it is shown in some OI types [28]. We think anomalies in *FKBP10* expression could be compared to other chaperone defects, causing recessive OI. Similarly to cases where CyPB is absent and the OI phenotype is less severe compared to deficiencies of P3H1 or CRTAP, a lack of FKBP65 could cause milder forms of OI than those due to HSP47 insufficiency [20]. Moreover, the possible mineralization defects we showed at the histomorphometry and the absence of limb pterygia, could confirm that *FKBP10* mutations can cause a form of OI not necessarily with arthrogryposis [29,30].

Concerning biological data, we do not report any alteration in the majority of bone metabolic markers ALP, PTH, 25OHD or calcium (except for CTX that has always remained above normal ranges, as it usually does in many OI patients). As far as the radiological aspects are concerned, our patients showed mild vertebral flattening, severe scoliosis and wormian bones in the skull, a feature otherwise present in the majority of the other FKBP10 mutated patients [29]. Evaluating the bone histology, we have to consider that the patient had been treated for 7 years with BP and that there is no published evidence that remodeling activity is restored to pre-treatment levels after stopping neridronate for 6 months; the mineralization defect we noticed if not due to direct BP effect on bone remodeling could be part of our patient condition. A constant increase in BMD, even if slighter than in OI types I, III and IV, was observed during the first 3 years of treatment with BP. GH treatment was helpful in bringing about a slight reactivation of the increasing BMD, but overall it seemed to stabilize the BMD. In fact, when it was suspended because of surgical intervention, BMD decreased, even though there was no change in the speed of growth. At any rate, BP treatment in our patient improved bone mineral mass and reduced fracture incidence, but with minor effects if compared with other types of OI under treatment [31]. Comparing our patient with the other known OI, he differs from both type III, by the relative wellbeing in the first years of life, and mild OI forms by the following clinical history and final bone deformations. The progressive moderate severity of his clinical evolution, the possible mineralization defect and the osteoporosis degree could resemble those of type VI. However, our patient ALP values are within the normal range and the other histomorphometric findings are not typical for OI type VI [5,31]. Lastly both the clinical history and the osteoporosis are less severe compared to other recessive OI forms, although extremely short stature (typical of types VII and VIII) also contributes to a very low z score on DXA (DXA z scores of −5.5 vs. average DXA z scores of −6 to −7 in types VII and VIII).

Procollagen I is a heterotrimer assembled in the lumen of the ER; chaperones such as PDI, BiP, GRP94, HSP47 and FKBP65 prevent premature association between procollagen chains and assist proper

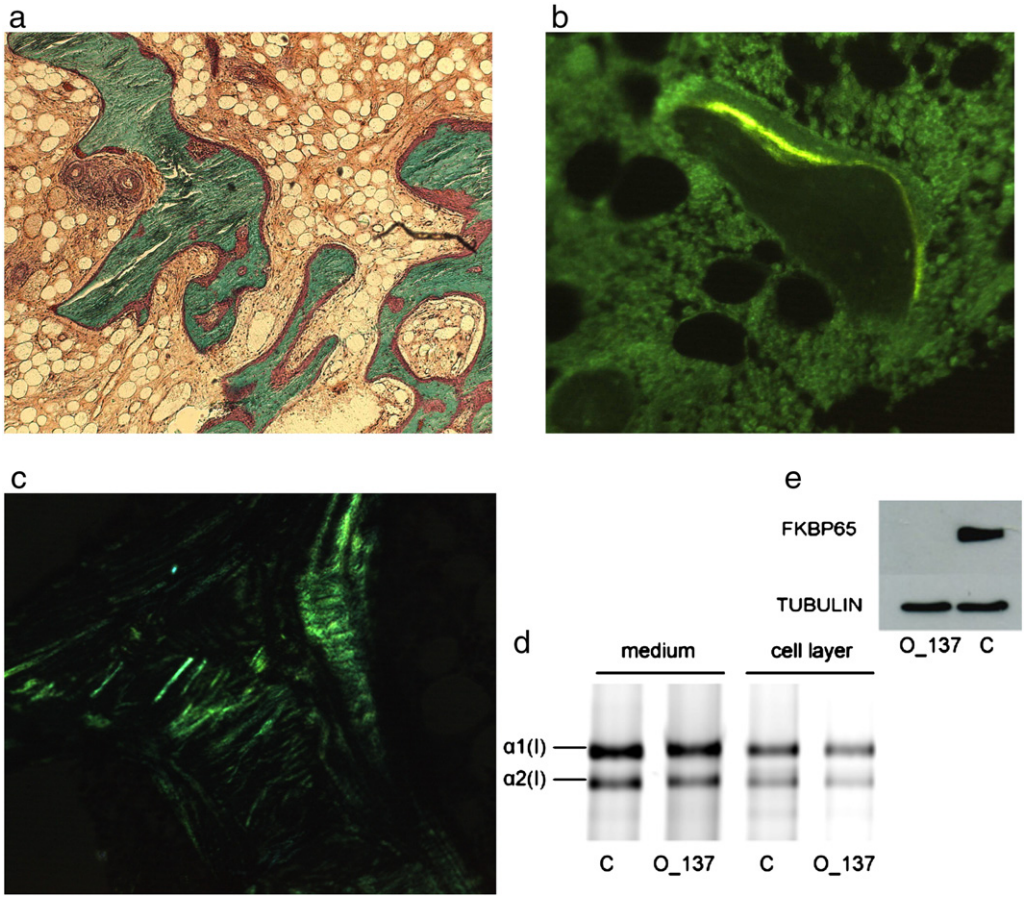

Fig 2. a–c. Histological sections from iliac crest of the affected individual showing a significant increase in both osteoid thickness and surface (a), revealing poor, diffuse uptake of the tetracycline labels under fluorescent light (b) and abnormal lamellar bone patterns under polarized light (c); d. Pepsin-digested type I collagen in the medium and cell layer of cultured dermal fibroblasts from O_137 and control. Migration of α1 and α2 chains is normal compared to a standard collagen type I protein. Relative amounts of secreted α1 and α2 chains in patient and control are identical; e. Western blot of FKBP65 and α-tubulin (as loading control) in patient and control fibroblasts. Two monoclonal antibodies (M02 3B5 and M13 2D4 clones — AbNova®) were used which gave analogous results. The image is representative of the two.

registration, folding into the collagen triple helix and subsequent trafficking [32,33].

To date, a small number of mutations in *SERPINH1* [20] and *FKBP10* [21,29] have been associated with moderate to lethal phenotypes, showing the important role of ER-resident chaperones in collagen biosynthesis and their effective involvement in the clinical manifestations of non-classic OI.

The splicing mutation found in our patient causes the production of two stable mRNA molecules whose translation could result in two different proteins, both missing the last PPI domain and the terminal 4 amino acids HEEL that represent the signal peptide for ER retention (Fig. 3d). Western blot analysis did not reveal any FKBP65 signal in the patient fibroblasts. Considering that the new termination codons fall in the final exons, it is plausible that both stable transcripts could by-pass the nuclear nonsense-mediated-decay mechanism (NMD) and the corresponding defective proteins were degraded.

As previously reported [21], the lack of FKBP65 leads to an accumulation of type I procollagen within the cells and to a delay in its secretion without evident changes of post-translational modifications towards collagenous molecules. In agreement with Alanay et al., electrophoresis of our patient type I procollagen (data not shown) and collagen (Fig. 2d) showed a normal pattern.

It has been proven that FKBP65 acts as a chaperone on collagen with effects comparable to HSP47, both of which prevent premature association of procollagen into triple helix and increasing its thermal stability [32]. At any rate, it is probable that a lack of FKBP65 function causes flaws in the correct synthesis of collagen and other ECM proteins (such as tropoelastin) at folding level and during their secretion into the extracellular matrix. In fact, in a manner similar to HSP47 null cells, the lack of FKBP65 has been shown to lead to a delay in procollagen I secretion and to the presence of its intracellular aggregates [21]. A defect in collagen fibrillogenesis has also been detected in these cells, giving rise to fibrils that are branched and thinner than normal [33].

Further studies on FKBP65 mutant cells are needed in order to highlight potential fibrillogenesis aberrations that could cause anomalous orientation of the lamellae at bone hystomorphology levels.

Table 1
Patient's histomorphometric data.

	Patient values	Reference values age 13 yrs [26]
Bone volume/tissue volume (%)	18.9	24.4 ± 4.3
Trabecular thickness (μm)	82	148 ± 23
Osteoid thickness (μm)	12.32	6.7 ± 1.7
Osteoid surface/bone surface (%)	28	22.1 ± 7.8
Osteoid volume/bone volume (%)	14	2.12 ± 1.00
Mineral apposition rate (μm/day)	0.41	0.87 ± 0.09
Bone formation rate ($\mu m^3/\mu m^2$/day)	0.03	0.037 ± 0.02
Activation frequency (#/year)	0.32	0.83 ± 0.35
Adjusted apposition rate (μm/day)	0.10	0.46 ± 0.10
Mineralization lag time (days)	122	14.5 ± 3.0
Erosion surface/bone surface (%)	16	14.9 ± 5.6
Osteoclast surface/bone surface (%)	2.4	0.94 ± 0.38

All thickness/depth results are corrected for obliquity of sections by multiplying by π/4.

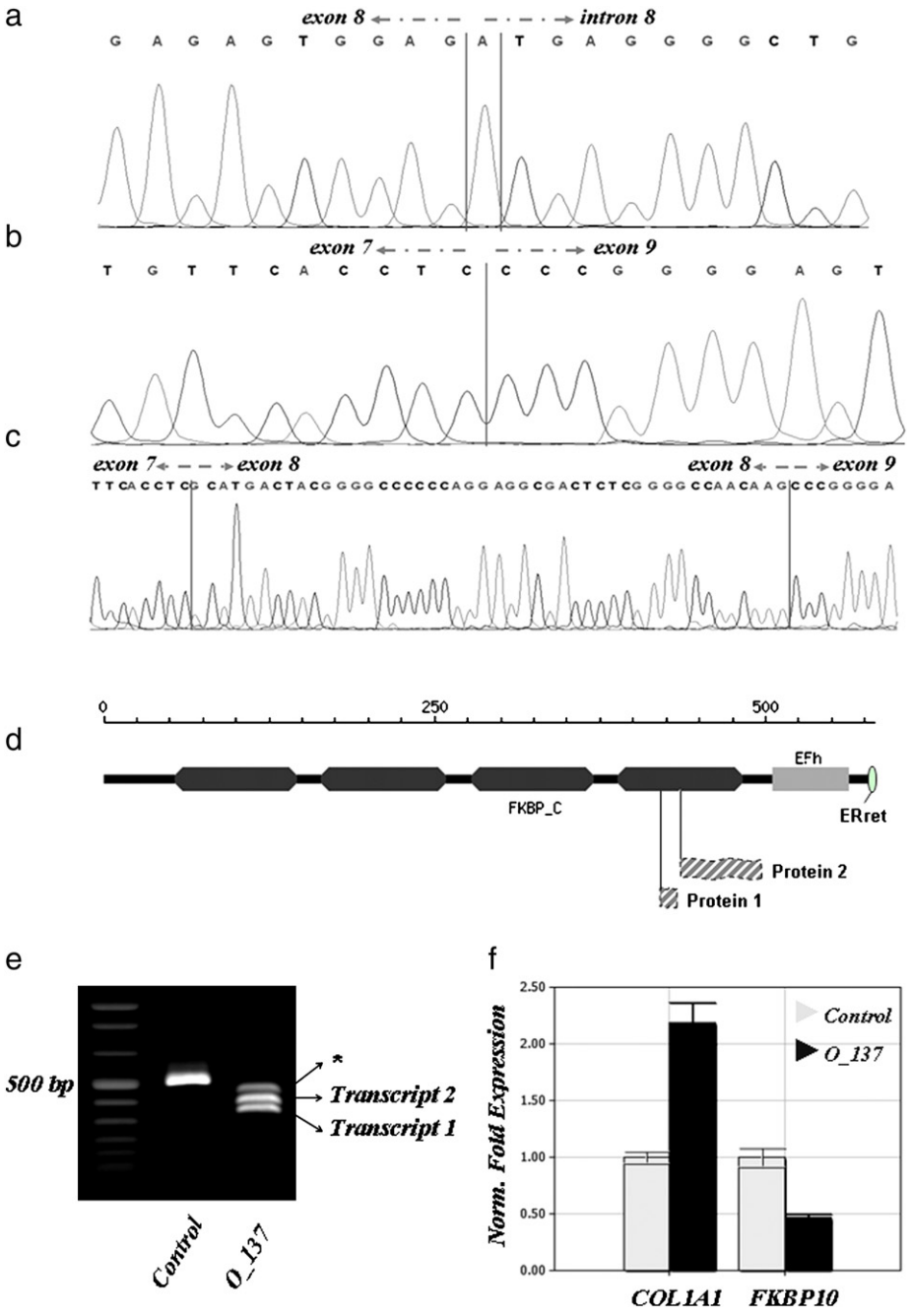

Fig 3. a. Patient's sequence of gDNA around the site of homozygous mutation IVS8+1G>A; the two vertical lines define base c.1399+1 (NM_021939.3) in the first strictly conserved position of the donor splicing site in intron 8. b. Patient's cDNA showing the sequence of transcript 1 with complete skipping of exon 8; vertical line defines last nucleotide of exon 7 from first nucleotide of exon 9. c. Sequence of exon 8 included in the mRNA of transcript 2 as a consequence of the activation of a cryptic donor splice site. Both transcripts 1 and 2 generate frameshift in the reading frame with the introduction of premature stop codons. d. Cartoon of the FKBP65 molecule and of two predicted proteins generated by the mutation. FKBP-type peptidyl-prolyl cis–trans isomerase; EF/Hand domain, calcium binding motif; ER-retention sequence. e. RT-PCR of *FKBP10* cDNA from control and O_137 showing the presence of two bands of 340 and 386 bp (483 bp wild type length) corresponding to two different transcripts; the third higher band (*) is an in vitro created heteroduplex between transcript 1 and 2 as demonstrated by its disappearance during 75 °C chromatographic separation in a DHPLC instrument (data not shown). f. qRT-PCR with relative expression levels of COL1A1 and FKBP10 mRNA in cultured fibroblasts normalized to GAPDH and HPRT1 used in combination as housekeeping genes. The experiments were repeated independently three times.

Acknowledgments

We wish to thank our patient and his family for their willingness and courtesy. We are grateful to Dr. Antonella Forlino, PhD, for her technical support and kind collaboration; we would also like to thank Dr. Maurizia Valli, PhD, for providing the patient's cell culture, Dr. Luca Donatelli, PhD, and Dr. Mirko Zanatta, MD, for their technical contributions. Finally, we are grateful to As.It.O.I. for its continuous support.

Appendix A. Supplementary data

Supplementary data to this article can be found online at doi:10.1016/j.bone.2011.10.023.

References

[1] Rauch F, Glorieux FH. Osteogenesis imperfecta. Lancet 2004;363:1377–85.
[2] Marini JC, Forlino A, Cabral WA, Barnes AM, San Antonio JD, Milgrom S, et al. Consortium for osteogenesis imperfecta mutations in the helical domain of type

I collagen: regions rich in lethal mutations align with collagen binding sites for integrins and proteoglycans. Hum Mutat 2007;28:209–21.
[3] Venturi G, Tedeschi E, Mottes M, Valli M, Camilot M, Viglio S, et al. Osteogenesis imperfecta: clinical, biochemical and molecular findings. Clin Genet 2006;70:131–9.
[4] Rauch F, Lalic L, Roughley P, Glorieux FH. Relationship between genotype and skeletal phenotype in children and adolescents with osteogenesis imperfecta. J Bone Miner Res 2010;25:1367–74.
[5] Glorieux FH, Ward LM, Rauch F, Lalic L, Roughley PJ, Travers R. Osteogenesis Imperfecta type VI: a form of brittle bone disease with a mineralization defect. J Bone Miner Res 2002;17:30–8.
[6] Baldridge D, Schwarze U, Morello R, Lennington J, Bertin TK, Pace JM, et al. CRTAP and LEPRE1 mutations in recessive osteogenesis imperfecta. Hum Mutat 2008;29:1435–42.
[7] Van Dijk FS, Pals G, Van Rijn RR, Nikkels PG, Cobben JM. Classification of osteogenesis imperfecta revisited. Eur J Med Genet 2010;53:1–5.
[8] Marini JC, Cabral WA, Barnes AM. Null mutations in LEPRE1 and CRTAP cause severe recessive osteogenesis imperfecta. Cell Tissue Res 2010;339:59–70.
[9] Lapunzina P, Aglan M, Temtamy S, Caparrós-Martín JA, Valencia M, Letón R, et al. Identification of a frameshift mutation in Osterix in a patient with recessive osteogenesis imperfecta. Am J Hum Genet 2010;87:110–4.
[10] Becker J, Semler O, Gilissen C, Li Y, Bolz HJ, Giunta C, et al. Exome sequencing identifies truncating mutations in human SERPINF1 in autosomal-recessive osteogenesis imperfecta. Am J Hum Genet 2011;88:362–71.
[11] Homan EP, Rauch F, Grafe I, Lietman C, Doll JA, Dawson B, et al. Mutations in SERPINF1 cause osteogenesis imperfecta type VI. J Bone Miner Res 2011 Aug 8, doi:10.1002/jbmr.487 [Epub ahead of print].
[12] Ward LM, Rauch F, Travers R, Chabot G, Azouz EM, Lalic L, et al. Osteogenesis imperfecta type VII: an autosomal recessive form of brittle bone disease. Bone 2002;31:12–8.
[13] Labuda M, Morissette J, Ward LM, Rauch F, Lalic L, Roughley PJ, et al. Osteogenesis imperfecta type VII maps to the short arm of chromosome 3. Bone 2002;31:19–25.
[14] Morello R, Bertin TK, Chen Y, Hicks J, Tonachini L, Monticone M, et al. CRTAP is required for prolyl 3-hydroxylation and mutations cause recessive osteogenesis imperfecta. Cell 2006;127:291–304.
[15] Barnes AM, Chang W, Morello R, Cabral WA, Weis M, Eyre DR, et al. Deficiency of cartilage-associated protein in recessive lethal osteogenesis imperfecta. N Engl J Med 2006;355:2757–64.
[16] Cabral WA, Chang W, Barnes AM, Weis M, Scott MA, Leikin S, et al. Prolyl 3-hydroxylase 1 deficiency causes a recessive metabolic bone disorder resembling lethal/severe osteogenesis imperfecta. Nat Genet 2007;39:359–65.
[17] Willaert A, Malfait F, Symoens S, Gevaert K, Kayserili H, Megarbane A, et al. Recessive osteogenesis imperfecta caused by LEPRE1 mutations: clinical documentation and identification of the splice form responsible for prolyl-3-hydroxylation. J Med Genet 2009;46:233–41.
[18] Barnes AM, Carter EM, Cabral WA, Weis M, Chang W, Makareeva E, et al. Lack of cyclophilin B in osteogenesis imperfecta with normal collagen folding. N Engl J Med 2010;362:521–8.
[19] van Dijk FS, Nesbitt IM, Zwikstra EH, Nikkels PG, Piersma SR, Fratantoni SA, et al. PPIB mutations cause severe osteogenesis imperfecta. Am J Hum Genet 2009;85:521–7.
[20] Christiansen HE, Schwarze U, Pyott SM, AlSwaid A, Al Balwi M, Alrasheed S, et al. Homozygosity for a missense mutation in SERPINH1, which encodes the collagen chaperone protein HSP47, results in severe recessive osteogenesis imperfecta. Am J Hum Genet 2010;86:389–98.
[21] Alanay Y, Avaygan H, Camacho N, Utine GE, Boduroglu K, Aktas D, et al. Mutations in the gene encoding the RER protein FKBP65 cause autosomal-recessive osteogenesis imperfecta. Am J Hum Genet 2010;86:551–9.
[22] Monti E, Mottes M, Fraschini P, Brunelli P, Forlino A, Venturi G, et al. Current and emerging treatments for the management of osteogenesis imperfecta. Ther Clin Risk Manage 2010;6:367–81.
[23] Glorieux FH. Experience with bisphosphonates in osteogenesis imperfecta. Pediatrics 2007;119:S163–5.
[24] Phillipi CA, Remmington T, Steiner RD. Bisphosphonate therapy for osteogenesis imperfecta. Cochrane Database Syst Rev 2008;4:CD005088.
[25] Forlino A, Kuznetsova NV, Leikin S. Selective retention and degradaton of molecules with a single mutant α 1(I) chain in the Brtl IV mouse model of OI. Matrix Biol 2007;26:604–14.
[26] Parfitt AM, Drezner MK, Glorieux FH, Kanis JA, Malluche H, Meunier PJ, et al. Bone histomorphometry: standardization of nomenclature, symbols, and units. J Bone Miner Res 1987;6:595–610.
[27] Glorieux FH, Travers R, Taylor A, et al. Normative data for iliac bone histomorphometry in growing children. Bone 2000;26:103–9.
[28] Shaheen R, Al-Owain M, Faqih E, Al-Hashmi N, Awaji A, Al-Zayed Z, et al. Mutations in FKBP10 cause both Bruck syndrome and isolated osteogenesis imperfecta in humans. Am J Med Genet A 2011;155:1448–52.
[29] Kelley BP, Malfait F, Bonafe L, Baldridge D, Homan E, Symoens S, et al. Mutations in FKBP10 cause recessive osteogenesis imperfecta and type 1 Bruck syndrome. J Bone Miner Res September 13 2010, doi:10.1002/jbmr.250 [published online ahead of print].
[30] Shaheen R, Al-Owain M, Sakati N, Alzayed ZS, Alkuraya FS. FKBP10 and Bruck syndrome: phenotypic heterogeneity or call for reclassification? Am J Hum Genet 2010;87:306–7.
[31] Land C, Rauch F, Travers R, Glorieux FH. Osteogenesis imperfecta type VI in childhood and adolescence: effects of cyclical intravenous pamidronate treatment. Bone 2007;40:638–44.
[32] Ishikawa Y, Vranka J, Wirz J, Nagata K, Bächinger HP. The rough endoplasmic reticulum-resident FK506-binding protein FKBP65 is a molecular chaperone that interacts with collagens. J Biol Chem 2008;283:31584–90.
[33] Ishida Y, Kubota H, Yamamoto A, Kitamura A, Bächinger HP, Nagata K, et al. collagen in Hsp47-null cells is aggregated in endoplasmic reticulum and deficient in N-propeptide processing and fibrillogenesis. Mol Biol Cell 2006;17:2346–55.